Electronic structure of hydrogenated-fluorinated a-$Si_{1-x}Ge_x$ alloys

Bal K. Agrawal and Savitri Agrawal
Department of Physics, Allahabad University, Allahabad 211 002, Uttar Pradesh, India
(Received 30 January 1987)

A very good description of the electron energy states in a-$Si_{1-x}Ge_x$:F(H) alloys has been obtained throughout the entire energy region in the cluster Bethe-lattice method for the first time. The calculation considers a high-energy excited s^* state in the basis of the atomic-orbital set. For a-$Si_{1-x}Ge_x$ alloys, the computed variations of the magnitude of the fundamental energy gap for the random and chemically ordered sequences are seen to be in excellent agreement with the available photoemission data. Great improvement in terms of the number and location of F-induced peaks in fluorinated a-Si alloy has been obtained where the calculated results are in very good agreement with the photoemission data. The F(H)-induced peaks remain unaffected by the presence of the different concentrations of the constituent host atoms in a-$Si_{1-x}Ge_x$ alloys both for the random and chemically ordered sequences.

I. INTRODUCTION

Improvement in the conversion efficiency of the amorphous silicon solar cell is the most important point for the practical application of the a-Si solar cell as an alternative nonconventional source of energy. A conversion efficiency of 11–12 % has recently been reached in Si-based devices in textured structures.[1] In an attempt to attain much higher conversion efficiency, multi-band-gap a-Si solar cells have to be developed. It stems from the fact that in contrast to the theoretical limit of maximum efficiency of 12.5–13 % for the conventional single-band-gap a-Si solar cell, multi-band-gap a-Si solar cell named tandem solar cell can have an estimated value of 21–24 %.[2]

Amorphous hydrogenated and/or fluorinated silicon-germanium alloys have energy gaps smaller than a-Si:H or a-Si:F:H. They have potential applications in tandem solar cells and also in electrophotography.

In recent years, several experimental measurements of the optical and electronic properties of the hydrogenated and/or fluorinated a-$Si_{1-x}Ge_x$ alloys have been reported in the literature.[3] However, no result of the measurement of the electronic density of states in the valence or conduction bands such as the photoemission experiments has been reported for these alloys. Also, the theoretical attempts on the a-$Si_{1-x}Ge_x$:F:H alloys are scarce. The lone calculation of Papaconstantopoulos *et al.*[4] for the electronic states for the Si:Ge-H alloys used a tight-binding Hamiltonian. Although these authors treated the diagonal disorder within the coherent-potential approximation, the authors made only a virtual-crystal approximation for the off-diagonal disorder. They assumed the occurrence of the H-H clusters in the calculation.

Our group is presently engaged in the theoretical study of the electron and phonon excitations of the amorphous semiconducting alloys containing H, F, and O atoms, etc. The results for the vibrational excitations for the a-$Si_{1-x}Ge_x$:F:H alloys are reported in another paper.[5]

In an earlier paper[6] one of the authors reported the results of the electronic structure of a cluster Bethe-lattice formalism for the a-$Si_{1-x}Ge_x$ alloys after considering all the nearest-neighbor interactions in a tight-binding Hamiltonian. The electrons on each atom were described by one s orbital and three p orbitals (p_x,p_y,p_z).

In all the cluster Bethe-lattice calculations considering nearest-neighbor atomic interactions, the main drawback has been the appearance of a electronic density of states (DOS) gap which is much wider as compared to the experimentally measured semiconducting gap.[7–9] Also, the electron states of the conduction band were not satisfactorily described by an sp^3 Hamiltonian. Improvement in terms of a comparatively smaller band gap has been achieved by inclusion of second-neighbor atomic interactions in pure a-Si alloy.[10] A successful attempt to remove these shortcomings has been made in the present paper. In order to have a better description of the conduction-band states similar to Vogl *et al.*,[11] we consider a high-energy state s^* at each atomic site and obtain the right values of the density-of-states gaps for the pure a-Si and a-Ge. The earlier calculation[6] for the a-$Si_{1-x}Ge_x$ alloys is revised and we now find a variation of the DOS gap with concentration x in excellent agreement with the available experimental data.[12–14] The calculations are then extended to the hydrogenated and the fluorinated a-$Si_{1-x}Ge_x$ alloys where the effects of the occurrence of the monohydride (fluoride) and dihydride (fluoride) complexes are investigated.

The inclusion of the high-energy s^* states does not merely make a surprising improvement in the values of the DOS gaps but also reduces the number of the calculated F-induced peaks induced by the difluoride complexes which are in excellent agreement with the photoemission data.

Section II contains a very brief account of the cluster Bethe-lattice method (CBLM) extended to the calculation of density of states in binary alloys. Two different types of the atomic arrangements, i.e., random sequence and the chemically ordered sequence in the alloys have been dis-

cussed. The results for the density of states of the a-$Si_{1-x}Ge_x$:H and a-$Si_{1-x}Ge_x$:F alloys are presented in Sec. III. The main conclusions are included in Sec. IV.

II. THEORY

A. LCAO scheme

For describing the electron states, we employ a linear combination of atomic orbital (LCAO) scheme where one usually employs a basis of four atomic orbitals (s,p_x,p_y,p_z). However, this orbital scheme suffers from the two main drawbacks: firstly the electronic states lying in the high-energy region, i.e., in the conduction band are not well described, and secondly, in a cluster Bethe-lattice calculation one usually obtains a density-of-states (DOS) gap which is much wider than the experimentally measured one. One way to circumvent the difficulty is the inclusion of a high-energy excited s-like state s^* in the basis set which improves the electron states especially in the lowest-energy conduction band in several semiconductors. We have thus considered a basis of the five orbital set (s,p_x,p_y,p_z,s^*) at each atomic site in our calculations which generate more reliable conduction states as well as the correct values of the DOS gaps in the elemental and III-V compound semiconductors[15] in agreement with the experimental values.

B. Interpolation scheme for A_xB_{1-x} alloys

In binary A_xB_{1-x} alloys, there are various probabilities of the occurrence of the A—A, A—B, B—A, and B—B bonds. We consider a reference site in the Cayley tree. The descendents of this reference site will be determined by the level of the valence saturation already present due to its parent atom. For an alloy having the same coordination for the two kinds of atoms, e.g., like $Si_{1-x}Ge_x$ alloys, let us assume that P_a (Q_a) is the probability of like (unlike) atom decendants of a A atom. The branching ratios of the descendants would be consistent with the saturation condition and the cluster averages for the different values of average probabilities. We consider the following three different sequences for describing the different bonding tendencies.

1. *Random sequence*

In this sequence any kind of atom has equal probability to saturate the valency of an atom compatible with the equal multiplicities. The probability of the occurrence of an atom is directly proportional to its concentration in the alloy. Thus, for a concentration x of atoms of kind A, one writes

$$P_a=x,\quad Q_a=1-x\ ;$$
$$P_b=1-x,\quad Q_b=x\ . \tag{1}$$

2. *Chemically ordered sequence*

In this sequence, atoms of small concentration are likely to be surrounded by the atoms of high concentration. Assuming atoms A present in small concentration x ($x<0.5$), we write

$$P_a=0,\quad Q_a=1\ ;$$
$$P_b=(1-2x)/(1-x),\quad Q_b=x/(1-x)\ . \tag{2}$$

If the atoms B are present in low concentration, x will be replaced by $(1-x)$ in Eq. (2).

3. *Segregation sequence*

In some alloys it is observed that like atoms cluster. This will result in the absence of any bond between unlike atoms, i.e., there are no A—B or B—A like bonds. The probabilities are then given by

$$P_a=P_b=1\ ,$$
$$Q_a=Q_b=0\ . \tag{3}$$

C. Cluster Bethe-lattice method

A Bethe lattice has been used for the calculation of the density of states. The local Green's function at any site can be calculated exactly. The density of states of the Bethe lattice is smooth and featureless, and therefore, the local environment of the atom leaves its signatures on the density of the energy states in a cluster Bethe-lattice calculation.

One may define the Green's-function operator denoted by $\underline{G}$ for a system by

$$\underline{G}=(\varepsilon\underline{I}-\underline{H})^{-1}\ , \tag{4}$$

where ε is energy of an excitation, $\underline{I}$ is the unit operator, and $\underline{H}$ is the Hamiltonian operator of the system. It may be rewritten as a Dyson equation in matrix form as

$$(\varepsilon\underline{I}-\underline{H}^0)\underline{G}=\underline{I}+\underline{V}\underline{G} \tag{5}$$

with

$$\underline{H}=\underline{H}^0+\underline{V}\ . \tag{6}$$

Here $\underline{H}^0$ is the diagonal matrix containing the energies of the noninteracting orbitals at the same site and $\underline{V}$ is the interaction Hamiltonian matrix between the orbitals lying on the different atoms, e.g., at the nearest-neighbor or the second-neighboring sites.

Once $\underline{G}$ is known, various properties of the system such as the electronic density of states can be calculated easily. The matrix elements of Eq. (5) can explicitly be written as

$$\varepsilon\langle i\mid\underline{G}\mid j\rangle=\underline{I}_{ij}+\sum_{k=1}^{4}\langle i\mid\underline{V}\mid k\rangle\langle k\mid\underline{G}\mid j\rangle\ . \tag{7}$$

Equation (7) can be solved exactly for a Bethe lattice. The infinite set of coupled equations can be reduced to a small set by utilizing the symmetries of the Bethe lattice in the form of the transfer matrices or the effective fields. And two nearest-neighboring dots are connected to each other by only one self-avoiding path. One can define a transfer matrix $\underline{t}_{ji}$ at site i for each inequivalent line (j) joining any two nearest-neighboring dots. By definition, the Green's function at one site should be identically

equal to one with the entire Bethe lattice. The Green's function between the two more distant sites i and k is related to that between the two nearest ones i and j by

$$\underline{G}_{ki}=\underline{t}_{kj}\underline{G}_{ji} , \tag{8}$$

where $\underline{t}_{kj}$ is the transfer matrix or the effective field at the site j along the direction of atom k. The local density of states at the atomic site (i) is

$$\rho_i(\varepsilon)=(-1/\pi)\mathrm{Im\,Tr}(\underline{G}_{ii}) , \tag{9}$$

where $\mathrm{Im\,Tr}(\underline{G}_{ii})$ is the imaginary part of the trace of the Green's-function matrix at the site i.

In the binary alloy A_xB_{1-x}, a particular kind of atom can have both kinds of neighbors. One needs to know the two different effective fields (transfer matrices) for each kind of reference atom. For the reference atom A one has the transfer matrices $\underline{t}_{aa}$ and $\underline{t}_{ba}$. Similarly, for the reference atom B, we should know $\underline{t}_{ab}$ and $\underline{t}_{bb}$. Thus for each lattice site, there are four unknown matrices. For the neighboring site, we denote the similar transfer matrices by

$$\underline{\bar{t}}_{aa},\ \underline{\bar{t}}_{ab},\ \underline{\bar{t}}_{ba},\ \text{and}\ \underline{\bar{t}}_{bb} .$$

The above unknown eight transfer matrices are related among themselves by the following eight self-consistent equations:

$$\begin{aligned}
\underline{t}^i_{aa} &= \left[E\underline{I}-\underline{H}^0_{aa}-P_a\sum_k{}'(\underline{V}^k_{aa})^T\underline{\bar{t}}^k_{aa}-Q_a\sum_k{}'(\underline{V}^k_{ab})^T\underline{\bar{t}}^k\right]^{-1}(\underline{V}^i_{aa})^T ,\\
\underline{\bar{t}}^i_{aa} &= \left[E\underline{I}-\underline{H}^0_{aa}-P_a\sum_j{}'\underline{V}^j_{aa}\underline{t}^j_{aa}-Q_a\sum_j{}'\underline{V}^j_{ab}\underline{t}^j_{ab}\right]^{-1}\underline{V}^i_{aa} ,\\
\underline{t}^i_{ab} &= \left[E\underline{I}-\underline{H}^0_{bb}-P_b\sum_k{}'(\underline{V}^k_{bb})^T\underline{\bar{t}}^k_{bb}-Q_b\sum_k{}'\underline{\bar{V}}^{k\,T}_{ba}\underline{\bar{t}}^k_{ba}\right]^{-1}(\underline{V}^i_{ba})^T ,\\
\underline{\bar{t}}^i_{ab} &= \left[E\underline{I}-\underline{H}^0_{bb}-P_b\sum_j{}'\underline{V}^j_{bb}\underline{t}^j_{bb}-Q_b\sum_j{}'\underline{V}^j_{ba}\underline{t}^j_{ba}\right]^{-1}\underline{V}^i_{ba} ,\\
\underline{t}^i_{bb} &= \left[E\underline{I}-\underline{H}^0_{bb}-P_b\sum_k{}'(\underline{V}^k_{bb})^T\underline{\bar{t}}^k_{bb}-Q_b\sum_k{}'(\underline{V}^k_{ba})^T\underline{\bar{t}}^k_{ba}\right]^{-1}(\underline{V}^i_{bb})^T ,\\
\underline{\bar{t}}^i_{bb} &= \left[E\underline{I}-\underline{H}^0_{bb}-P_b\sum_j{}'\underline{V}^j_{bb}\underline{t}^j_{bb}-Q_b\sum_j{}'\underline{V}^j_{ba}\underline{t}^j_{ba}\right]^{-1}\underline{V}^i_{bb} ,\\
\underline{t}^i_{ba} &= \left[E\underline{I}-\underline{H}^0_{aa}-P_a\sum_k{}'(\underline{V}^k_{aa})^T\underline{\bar{t}}^k_{aa}-Q_a\sum_k{}'(\underline{V}^k_{ab})^T\underline{\bar{t}}^k_{ab}\right]^{-1}(\underline{V}^i_{ab})^T ,\\
\underline{\bar{t}}^i_{ba} &= \left[E\underline{I}-\underline{H}^0_{aa}-P_a\sum_j{}'\underline{V}^j_{aa}\underline{t}^j_{aa}-Q_a\sum_j{}'\underline{V}^j_{ab}\underline{t}^j_{ab}\right]^{-1}\underline{V}^i_{ab} .
\end{aligned} \tag{10}$$

Here $\underline{t}^i_{aa}$ $(\underline{\bar{t}}^i_{aa})$, $\underline{t}^i_{ab}$ $(\underline{\bar{t}}^i_{ab})$, $\underline{t}^i_{ba}$ $(\underline{\bar{t}}^i_{ba})$, and $\underline{t}^i_{bb}$ $(\underline{\bar{t}}^i_{bb})$ are the transfer matrices along the $A-A$, $B-A$, $A-B$, and $B-B$ bonds, respectively, in the direction i and $\sum'$ denotes summation over all the nearest neighbors of an atom except the one in the direction i.

The local Green's functions at Ge and Si atoms are, respectively,

$$\begin{aligned}
\underline{G}_{aa} &= \left[E\underline{I}-\underline{H}^0_{aa}-P_a\sum_{j=1}^4\underline{V}^j_{aa}\underline{t}^j_{aa}-Q_a\sum_{j=1}^4\underline{V}^j_{ab}\underline{t}^j_{ab}\right]^{-1} ,\\
\underline{G}_{bb} &= \left[E\underline{I}-\underline{H}^0_{bb}-P_b\sum_{j=1}^4\underline{V}^j_{bb}\underline{t}^j_{bb}-Q_b\sum_{j=1}^4\underline{V}^j_{ba}\underline{t}^j_{ba}\right]^{-1} .
\end{aligned} \tag{11}$$

III. CALCULATIONS AND RESULTS

The values of the various interaction integrals appearing in the LCAO scheme are included in Tables I and II. The high-energy excited s^* site of an atom is allowed to interact with the p orbitals of the neighboring atoms via the integral $\langle s^*\,|\,H\,|\,p\rangle=H$. The value of this integral is

TABLE I. Atomic-orbital energies measured with respect to the top of the valence band in eV.

Orbitals	Si	Ge	H	F
E_{s^*}	7.27	6.58		3.19
E_p (E_{p^*})	2.30	2.16	6.7	−9.3
E_s	−3.95	−5.1	−3.38	−28.1

TABLE II. Values of the first-neighbor and second-neighbor matrix elements for the interaction matrix for the different bonds in eV.

Interaction	Bond	U	X	V	T	H
First neighbor	Si—Si	−1.94	1.01	1.73	0.66	0.88
	Ge—Ge	−1.79	0.93	1.60	0.61	0.85
	Si—Ge	−1.87	0.97	1.67	0.64	0.87
	Si—F	−9.42	2.94	3.73	0.34	1.46
	Si—H	−3.43	1.31	0.82	0.82	0.65
	Ge—F	−8.68	2.7	3.4	0.31	1.34
	Ge—H	−3.16	1.20	0.76	0.76	0.60
Second neighbor	F—Si—F	3.47	−0.13	0.85	0.60	−0.64
	F—Ge—F	3.20	−0.12	0.78	0.55	−0.59
	F—Si	1.74	−0.065	0.30	0.50	−0.032
	F—Ge	1.60	−0.060	0.27	0.46	−0.030
	H—Si	0.25		0.15	0.15	
	H—Ge	0.23		0.14	0.14	
	H—Si—H	0.51		0.31	0.31	
	H—Ge—H	0.47		0.28	0.28	

fitted to match the calculated DOS gap with the experimental gaps for a-Si and a-Ge.

A. a-$Si_{1-x}Ge$ alloys

The computed local electron density of states for the pure a-Ge and a-Si are presented in Fig. 1. The magnitudes of the fundamental gaps for Ge and Si are reproduced as 1.1 and 1.8 eV, respectively, which are equal to the experimentally measured values.

For the calculation of the density of states for a-$Si_{1-x}Ge_x$ alloy, we employ the mean values of the nearest-neighbor interaction integrals used earlier for the pure a-Si and a-Ge in bulk. The calculations have been performed both for the random and chemically ordered sequences. The main features are the same as discussed in an earlier paper[6] barring the fact that now the magnitude of the fundamental gap E_g for a $Si_{1-x}Ge_x$ alloy is in agreement with the experimental data. The variation of E_g with the concentration x for the random and the chemically ordered alloys is compared with the experimental points in Fig. 2. The available experimental data from the three groups[12–14] are in excellent agreement with the calculated results. The variation of E_g is seen to be slightly different for the random and the chemically ordered sequences.

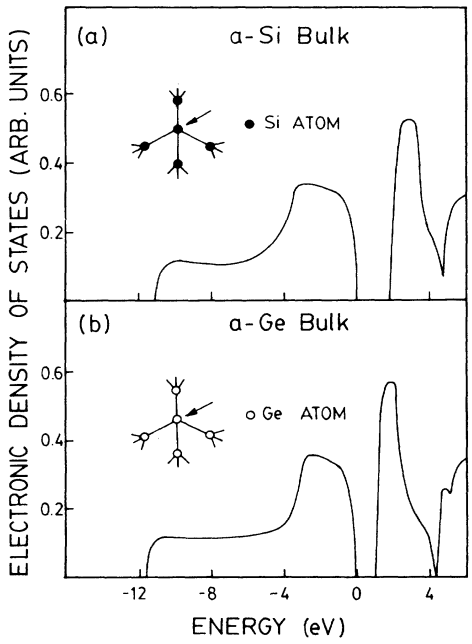

FIG. 1. Electronic density of states for (a) Si and (b) Ge Bethe lattices.

B. a-$Si_{1-x}Ge_x$:F alloys

1. *SiF and SiF_2 units*

We study the effects of the presence of the monofluorides and difluorides, SiF and SiF_2, on the elec-

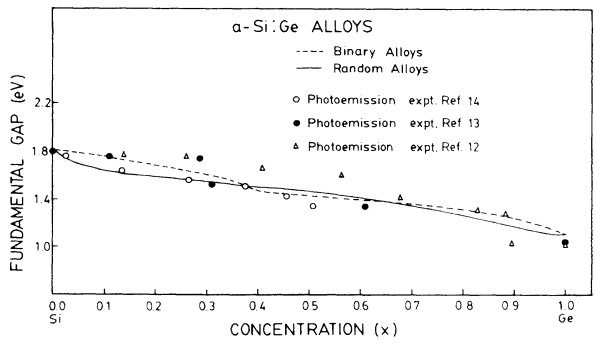

FIG. 2. Comparison of variation of the fundamental gap in a-$Si_{1-x}Ge_x$ alloys calculated for the binary and random sequences with the photoemission data.

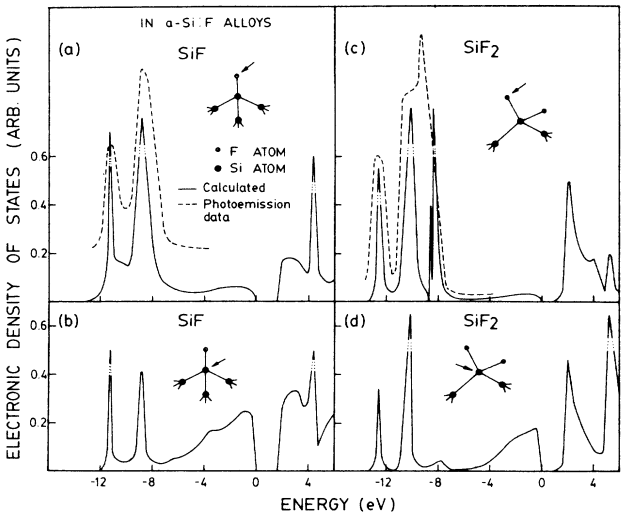

FIG. 3. Local electronic density of states for SiF_n $(n=1,2)$ units in a-Si:F alloys.

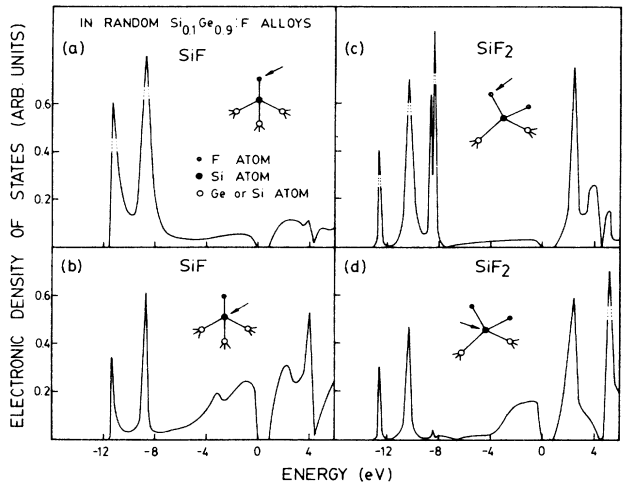

FIG. 4. Local electronic density of states for SiF_n $(n=1,2)$ units in random a-$Si_{0.1}Ge_{0.9}$:F alloys.

TABLE III. Calculated peaks for the various conformations in a-$Si_{1-x}Ge_x$ random and chemically ordered alloys in eV.

Concentration x	Conformation	Peaks Calculated (chemically ordered)	Peaks Calculated (random)	Expt. (in a-Si:H or Si:F alloys)
$x=0.1$	GeF	−11.1	−11.2	
		−8.6	−8.6	
	GeF_2	−12.4	−12.5	
		−10.2	−10.1	
		−8.6	−8.6	
		−8.4	−8.4	
	GeH	−10.0	−10.2	
		−4.0	−4.0	
	GeH_2	−10.0	−10.6	
		−6.2	−6.2	
$x=0.9$	SiF	−11.3	−11.3	−11.3
		−8.8	−8.7	−8.9
	SiF_2	−12.6	−12.6	−12.5
		−10.3	−10.4	−10.2
		−8.6	−8.6	
		−8.4	−8.4	−9.2
	SiH	−9.3	−9.3	−10.3
		−7.2	−7.2	−7.6
		−4.0	−4.0	−5.3
	SiH_2	−10.4	−6.4	−11.3
		−6.5	−6.5	−6.3

tronic structure of the a-$Si_{1-x}Ge_x$ alloys both for the random and chemically ordered sequences. The atomic orbital energies (Table I) for F atoms have been shifted by 1.8 eV for SiF and by 0.9 eV for SiF_2 units. For elucidating these effects, one needs to know the effects of these complexes on the structure of the pure a-Si and a-Ge alloys. Earlier[8,9] we reported the results within the four orbital basis (s,p_x,p_y,p_z). After employing the new basis of five orbitals (s,p_x,p_y,p_z,s^*) the calculations have been performed again and the results for the random sequence are shown in Fig. 3.

For SiF complex in pure a-Si, the salient features in the local density of states remain the same. However, for the case of difluoride (SiF_2), the features are drastically altered. In place of the five peaks obtained earlier[8] with a four orbital basis, we now obtain only three peaks appearing at -12.6 and -10.1, and -8.5 (-8.6 and -8.4) eV. These values are very close to the experimentally observed three peaks appearing at -12.5, -10.2, and -9.2 eV in the photoemission data.[16] Thus, a spectacular improvement is achieved with the new five orbital basis. The results for the chemically ordered sequences are similar.

The calculations have then been performed for the SiF and SiF_2 complexes present in a-$Si_{1-x}Ge_x$ alloy for different concentrations. The locations of the F-induced peaks by SiF and SiF_2 units are not distributed much by the other kind of atoms, i.e., Ge atoms when they are present as the other nearest neighbors of the reference Si atom coupled to the F atoms. As a typical case, we present here the local density of states at F and Si atoms for the random a-$Si_{0.1}Ge_{0.9}$ alloy in Fig. 4. A comparison of the locations of the calculated peaks obtained for the random and chemically ordered sequence with the photoemission ones has been made in Table III.

For the Si-F unit in the $Si_{0.1}Ge_{0.9}$ alloy, where the number of the Ge atoms are in a large majority, the new peak positions are -11.3 and -8.7 eV as compared to their locations at -11.3 and -8.9 eV in pure a-Si. Similarly, for the SiF_2 complex the three peaks appearing at -12.6, -10.3, and -8.5 eV in the $Si_{0.1}Ge_{0.9}$ alloy are similar to their locations at -12.6, -10.1, and -8.5 eV in the pure a-Si.

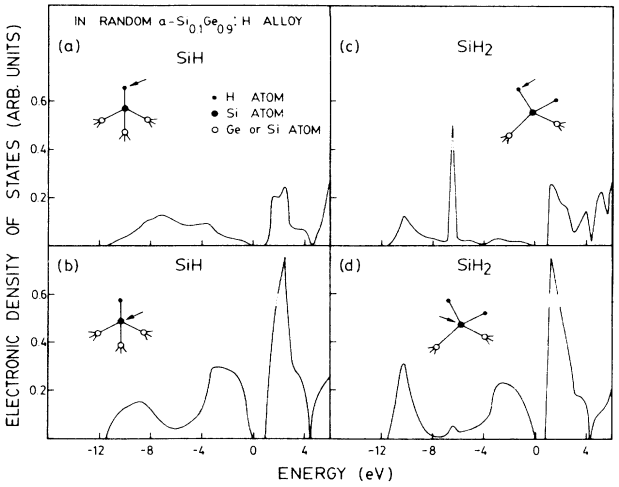

FIG. 6. Electronic density of states for SiH_n ($n=1,2$) units in random a-$Si_{0.1}Ge_{0.9}$:H alloys.

2. *SiH and SiH_2 units*

The atomic orbital energies (Table I) for H atoms have been shifted by -0.85 eV for SiH and by -1.7 eV for SiH_2 units. The local density of states for the monohydride (SiH) and dihydride (SiH_2) units in pure a-Si is depicted in Fig. 5. The features remain unchanged after the consideration of the high-energy s^* state. Also, the locations of the H-induced peaks are mostly unaffected. For SiH, the H-induced peaks which appear at -9.3 and -4.0 eV in pure a-Si are seen to appear practically at the same location in the a-$Si_{0.1}Ge_{0.9}$ alloy (see Fig. 6) whereas for SiH_2, the two peaks appearing at -10.4, and -6.4 eV in the pure a-Si occur at the same locations in the $Si_{0.1}Ge_{0.9}$ alloy (see Table III). Again, the results for the chemically ordered alloys are similar to those obtained for the random atomic configuration.

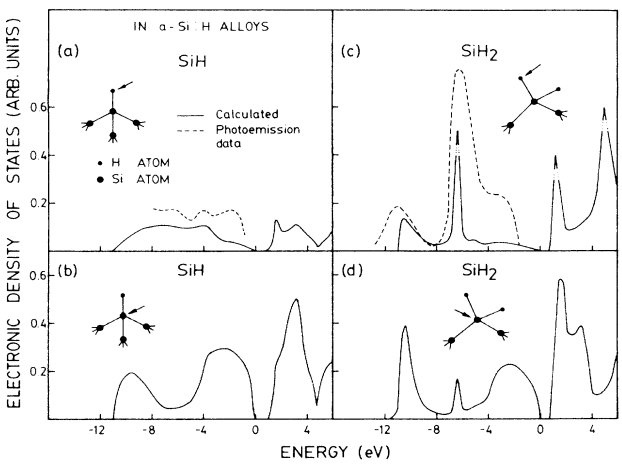

FIG. 5. Electronic density of states for SiH_n ($n=1,2$) units in random a-Si:H alloys.

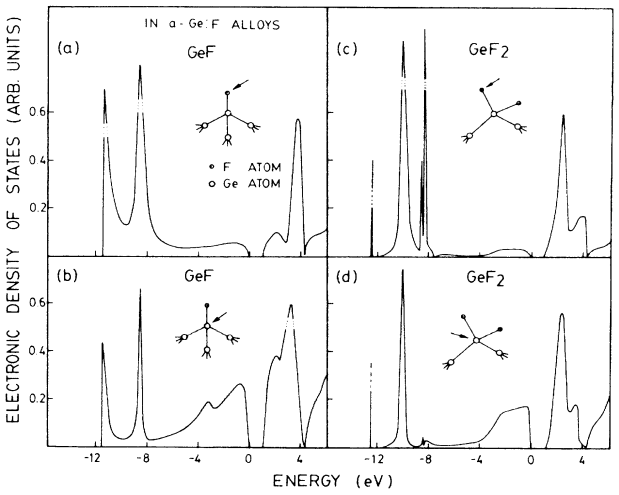

FIG. 7. Electronic density of states for GeF_n ($n=1,2$) units in a-Ge:F alloys.

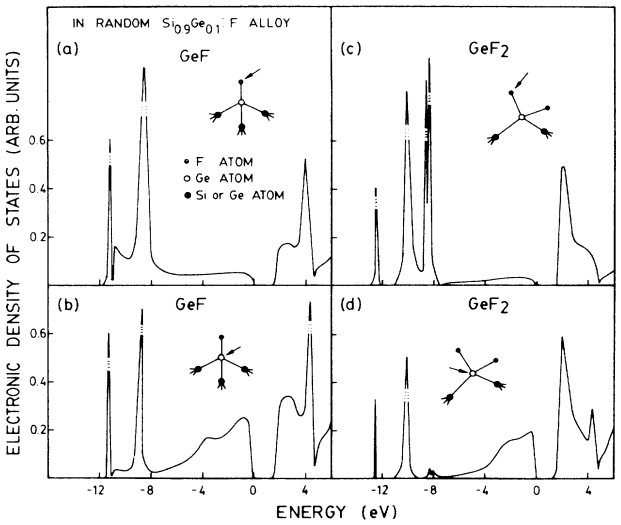

FIG. 8. Electronic density of states for GeF_n ($n=1,2$) units in random a-$Si_{0.9}Ge_{0.1}$:F alloys.

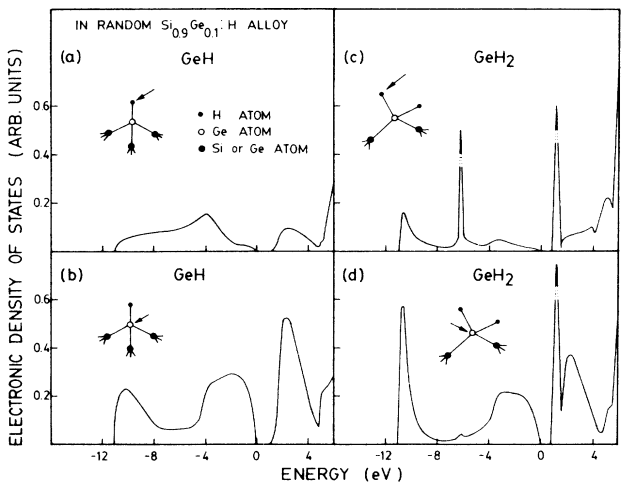

FIG. 9. Electronic density of states for GeH_n ($n=1,2$) units in random a-$Si_{0.9}Ge_{0.1}$:F alloys.

3. *GeF and GeF_2 units*

The new features arising from the inclusion of s^* state in the calculation are very much similar to those seen earlier for the SiF and SiF_2 complexes. The local density of states is presented in Fig. 7. The three peaks caused by the presence of GeF_2 unit appear at -12.5, -10.1, and -8.5 eV in contrast to the appearance of five peaks reported earlier[9] in the calculation considering only the four orbital basis. No experimental data are available for the a-Ge:F alloys.

Again, the presence of Si atoms as the neighbors of the Ge atom coupled to F atoms do not affect the F-induced peaks in a $Si_{0.9}Ge_{0.1}$:F alloy (see Fig. 8).

4. *GeH and GeH_2 units*

The calculated electronic density of states for GeH and GeH_2 units in the a-$Si_{0.9}Ge_{0.1}$ alloy in random sequence have been depicted in Fig. 9. Arguments similar to the other unit described above are also valid for them. The locations of the peaks for the random and chemically ordered a-$Si_{0.9}Ge_{0.1}$:H alloys are included in Table III.

IV. CONCLUSIONS

The present study reveals that the CBLM is quite capable of furnishing a very reliable description of the electron-energy states throughout the entire energy region. The consideration of the high-energy s^* states in the elemental and compound semiconductors reproduce the experimentally measured values for the energy gap. Further, a much better description of the F-induced peaks in a-Si has been obtained which is in excellent agreement with the photoemission data both in the number and the location of peaks. Finally, the H- and F-activated peaks in a-$Si_{1-x}Ge_x$ alloys both in the random and chemically ordered atomic configurations remain unaffected by the process of the other kind of atoms in these alloys. Photoemission measurements need to be performed on the a-$Si_{1-x}Ge_x$:F(H) alloys.

ACKNOWLEDGMENTS

The authors acknowledge the financial assistance from the Department of Science and Technology, Government of India, New Delhi.

[1]Y. Kuwano, Tech. Dig. **1**, 13 (1984).
[2]S. Tsuda *et al.*, Jpn. J. Appl. Phys. **21**, Suppl. **21-2**, 251 (1985).
[3]For several papers see, J. Non-Cryst. Solids **77&78**, (1985).
[4]D. A. Papaconstantopoulos, E. N. Economu, and A. D. Zoletsis, *Proceedings of XVII, International Conference on Physics of Semiconductors, San Franscico, 1984,* edited by J. D. Chadi and W. A. Harrison (Springer-Verlag, Berlin, 1985).
[5]Bal K. Agrawal, B. K. Ghosh, and P. S. Yadav (unpublished).
[6]Bal K. Agrawal, Phys. Rev. B **22**, 6294 (1980); **26**, 5972 (1982).
[7]J. D. Joannopoulos and F. Yndurain, Phys. Rev. B **10**, 5164 (1974).
[8]Bal K. Agrawal and Savitri Agrawal, Phys. Rev. B **29**, 6870 (1984).
[9]S. Agrawal and Bal K. Agrawal, Phys. Rev. B **31**, 5355 (1985); J. Phys. C **19**, 2741 (1986).
[10]D. C. Allan, W. B. Pollard, and J. D. Joannopoulos, Phys. Rev. B **25**, 1065 (1982).
[11]P. Vogl, Harold P. Hjalmarson, and John D. Dow, J. Phys. Chem. Solids **44**, 365 (1983).
[12]B. Von Roeden, D. K. Paul, J. Blake, R. W. Collins, G. Modolel, and W. Paul, Phys. Rev. B **25**, 7678 (1982).
[13]W. Beyer, H. Wagner, and F. Finger, J. Non-Cryst. Solids **77&78**, 857 (1985).
[14]K. D. Mackenzie, J. Hanna, J. R. Eggert, Y. M. Li, Z. L. Sun, and W. Paul, J. Non-Cryst. Solids **77&78**, 881 (1985).
[15]Bal K. Agrawal and Savitri Agrawal, Phys. Rev. B **34**, 4167 (1986).
[16]L. Ley, H. R. Shanks, C. J. Fang, K. J. Gruntz, and M. Cardona, Phys. Rev. B **15**, 6140 (1980).